Program Digest, 2019 IEEE International Ultrasonics Symposium (IUS)
Glasgow, Scotland, October 6-9, 2019

Low Velocity I.H.P. SAW Using Al/Pt Electrodes for Miniaturization

Ryo Nakagawa[1], Hideki Iwamoto[1], and Tsutomu Takai[1]
[1]Murata Manufacturing Co., Ltd., Kyoto, Japan

***Abstract*— In this paper, we study a velocity reduction of incredible high performance (I.H.P.) surface acoustic wave (SAW). First, variations of I.H.P. SAW velocity and fractional bandwidth with thickness of Pt layer in Al/Pt electrode are estimated using a finite element method simulator, and specific conditions where the SAW velocity can be reduced maintaining the fractional bandwidth equivalent to that of the conventional structure are determined. Then some one-port resonators under the determined conditions are fabricated and their velocity, fractional bandwidth, quality factor, and temperature stability are evaluated. As the result, it is indicated that, by using Al/Pt electrode and by adjusting the film thicknesses of a multilayer substrate, the velocity of I.H.P. SAW is successfully reduced while keeping other important characteristics.**

I. INTRODUCTION

Multilayer substrates for surface acoustic wave (SAW) devices have been paid much attentions since they have great potential to improve many important characteristics of SAW devices such as quality factor, temperature stability, and electromechanical coupling. The first report of this potential is by some of the authors in 2016[1]. In the report, a structure consist of thin $LiTaO_3$ (LT) and SiO_2 film and acoustic mirror was employed, and marked improvement of the Bode-Q[2], temperature stability, and the bandwidth compared with the conventional leaky SAW were confirmed experimentally. The proposed wave mode traveling guided in a very thin piezoelectric layer was named incredible high performance (I.H.P.) SAW. After the report, many studies concerning to similar structures for further characteristics improvement of SAW devices have been reported in this several years[3-9].

In addition to these main characteristics, another strong concern for SAW devices is their sizes. In particular, for a use case as low band filters or duplexers/multiplexers, size reduction of each SAW chip without deteriorations of other important characteristics is strictly demanded.

As the one solution for the miniaturization of SAW chip size, the technique for velocity reduction using heavy metals for electrodes has been proposed for Rayleigh SAW on $LiNbO_3$ substrate[10,11]. Since the wavelength of SAW is proportional to the velocity in a fixed frequency, velocity reduction is directory lead to the downsizing of a interdigital transducer (IDT).

In this work, on the basis of the same approach, we attempt to reduce the velocity of I.H.P. SAW using heavy Al/Pt electrode while keeping other important main characteristics.

First, using a finite element method (FEM) simulator, impedance characteristics of I.H.P. SAW resonators with various electrode thickness, and substrate film (LT and SiO_2) thickness are calculated, and from the calculated data, the SAW velocity at the resonance frequency and the fractional bandwidth are estimated, and specific conditions where the velocity can be reduced keeping the fractional bandwidth equivalent to that in the conventional structure. Then, on the basis of this estimation, several one-port resonators are fabricated and their velocities, bandwidths, Bode-Qs, and temperature coefficients of frequency (TCFs) are evaluated.

II. CONVENTIONAL I.H.P. SAW STRUCTURE

Fig. 1 shows the conventional I.H.P. SAW structure proposed in 2017[12]. This structure is constructed by a multilayer substrate and IDT Al electrodes on it. The multilayer substrate consists of very thin 50°YX-LT (50LT) and SiO_2 film, and a support substrate of Si. Thicknesses of Al, LT, and SiO_2 layers are 7.3%, 30.0%, and 33.7% in the wavelength ratio, respectively. The wavelength is defined by the period of the IDT grating.

Fig. 2 shows the impedance characteristics of one pair electrodes in conventional I.H.P. SAW when the wavelength is 2.0 μm simulated by the FEM model mentioned in the next section. In this case, the velocity of the SAW in the structure is approximately 3800 m/s.

In this work, to reduce the velocity of the SAW by heavy electrode, a Pt layer is inserted between the Al electrode and the LT film. In addition, the LT and the SiO_2 thicknesses are adjusted to keep the other characteristics such as the bandwidth.

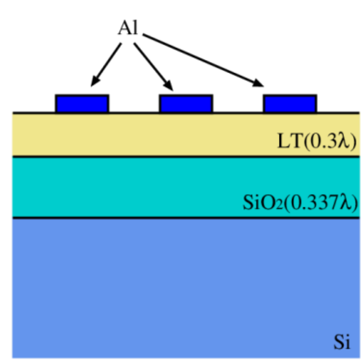

Fig. 1. Conventional I.H.P. SAW structure.

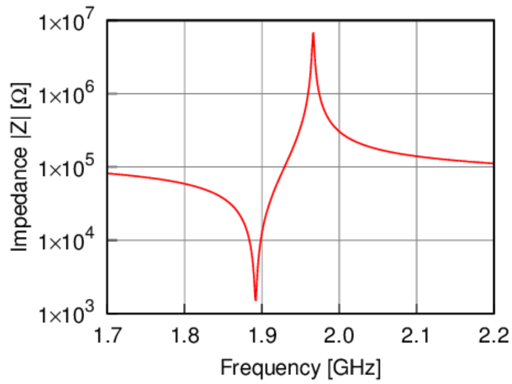

Fig. 2. Simulated impedance characteristics of conventional I.H.P. SAW.

III. FEM SIMULATION

Fig. 3 shows the simulation model for 2D-FEM used in this work. This model is constructed by a pair of electrode fingers composed of Al and Pt layers and 50LT/SiO_2/Si substrate. In addition, applying the periodic boundary condition to the each side of the substrate body, this model is assumed to be a part of the infinitely long IDT structure. Metallization ratio of the grating electrode is 0.5. Thicknesses of Al, LT, and SiO_2 layers are 7.3%, 30.0%, and 33.7% in the wavelength ratio, respectively, and the values are identical with the conventional I.H.P. SAW structure. Using this model, variations of the SAW velocity and the fractional bandwidth of a resonator with respect to the Pt, LT, and SiO_2 thickness are estimated.

First, calculated data of the SAW velocity at the resonance frequency normalized by the velocity when the Pt layer is not added and the fractional bandwidth with the variation of the Pt thickness is shown Figs. 4(a) and 4(b). In Fig. 4(a), the SAW velocity decreases monotonically with increase of the Pt thickness. This is due to the mass loading effect by the added Pt layer. When Pt thickness is 4.0% in wavelength ratio, SAW velocity is expected to be reduced approximately 20%. On the other hand, the fractional bandwidth becomes smaller compared with that of the conventional structure when the Pt thickness is larger than 2.0%. This degradation is not acceptable for the replacement of the conventional normal I.H.P. SAW (NM-I.H.P.).

Next, variation of the normalized SAW velocity and the fractional bandwidth with respect to the LT and SiO_2 thicknesses, where the Pt thickness in wavelength ratio is 4.0%, is shown in Figs. 5(a) and 5(b). In this calculation, LT and SiO_2 thicknesses are reduced while keeping their ratio. In this results, variation of the velocity is very small. On the other hand, the fractional bandwidth becomes large with decrease of the LT and SiO_2 thicknesses, and the variation is large enough to recover the degradation of the bandwidth due to the influence of the Pt layer.

Another technique to compensate the degradation of the bandwidth is alteration of the cut angle of piezoelectric layer. In Figs. 6(a) and 6(b), variation of the SAW velocity and the bandwidth with the cut angle are shown. This result show that, by using the low cut angle, the bandwidth become larger while keeping the SAW velocity. However, it is known that variation

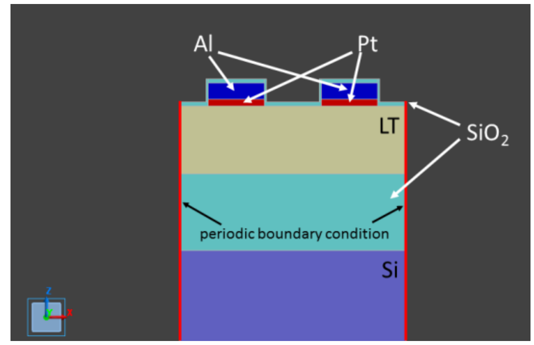

Fig. 3. Simulation model for 2D-FEM.

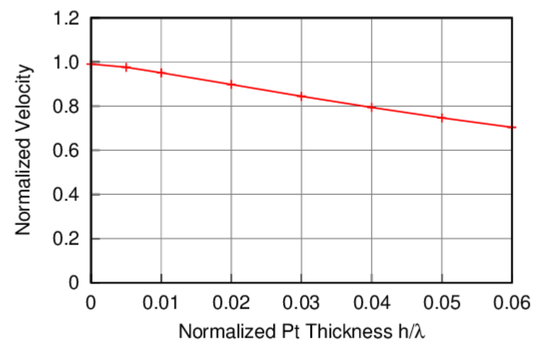

(a) Velocity

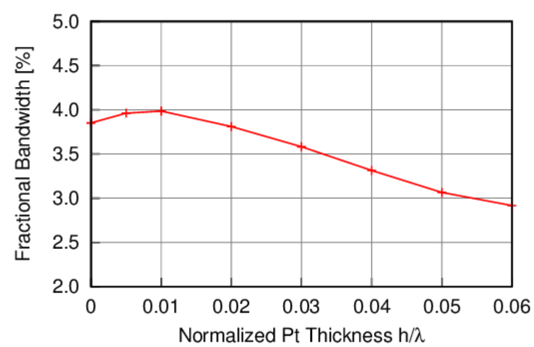

(b) Bandwidth

Fig. 4. Variation of velocity and fracdtional bandwidth with Pt thickness.

of the cut angle affects the temperature characteristics and the TCF is deteriorated when the low cut angle is employed[13]. Therefore, the bandwidth is better to be compensated not by the cut angle but by the thickness of the LT and SiO_2 layer.

IV. EXPERIMENTAL EVALUATION

On the basis of the calculation data in Sect. II, two one-port SAW resonators are fabricated and their characteristics are evaluated. Structure parameters of the fabricated resonators are shown in Table. I.

The structure of the resonator 1 is the conventional type and that of the resonator 2 is proposed for the low velocity I.H.P. SAW (LV-I.H.P.). In these structures, actual thicknesses

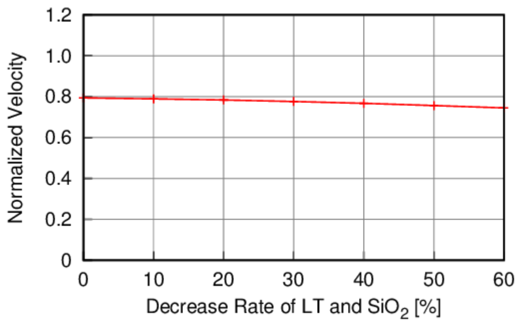

(a) Velocity

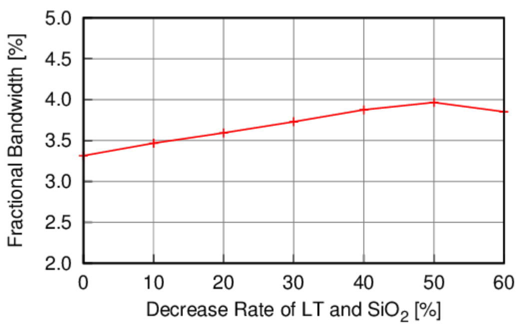

(b) Bandwidth

Fig. 5. Variation of velocity and fracdtional bandwidth with LT and SiO2 thickness.

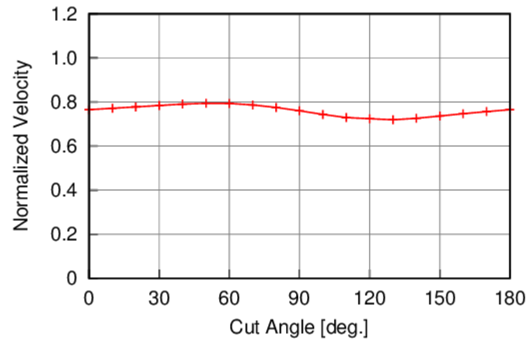

(a) Velocity

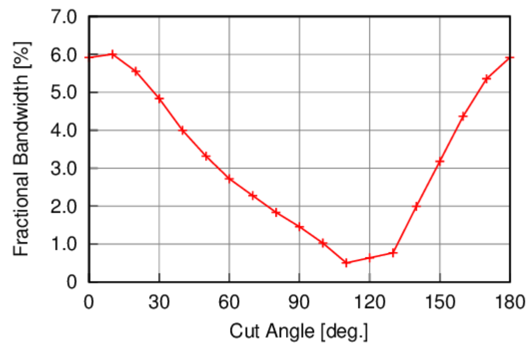

(b) Bandwidth

Fig. 6. Variation of velocity and fracdtional bandwidth with cut angle of LT.

of the substrate layers are fixed and the thicknesses in the wavelength ratio are adjusted by the grating period of the IDT on the substrate.

Figs. 7(a) and 7(b) show the measured impedance characteristics and Bode-Q of the fabricated resonators. In these figures, the red lines show the NM-I.H.P. of the resonator 1 and the blue lines show the LV-I.H.P. of the resonator 2 with Al/Pt electrodes. The horizontal axis shows the frequency normalized by the resonance frequency of the resonator 1 f_{r1} and the wavelengths of resonator 1 λ_1 and measured resonator λ using the equation below:

$$f_{\text{norm}} = \frac{f\lambda}{f_{r1}\lambda_1} \tag{1}$$

It is indicated in Fig. 7(a) that, by employing heavy Al/Pt electrodes, the velocity of the LV-I.H.P. in the resonator 2 is successfully reduced approximately 20% at the resonance frequency compared with the NM-I.H.P. in the resonator 1 as expected. In addition, Bode-Q of the LV-I.H.P. is not deteriorated or seems to be improved somewhat at the maximum point compared with the NM-I.H.P. in Fig. 7(b).

Table II shows the measured values of the fabricated resonators. The fractional bandwidth of LV-I.H.P. is also not deteriorated as estimated by the FEM simulations. With regard to the TCF, the absolute values at the resonance and anti-resonance frequencies are slightly larger than those of NM-I.H.P. This is probably due to the reduction of the thickness of the SiO_2 layer which has the temperature compensation feature.

TABLE I. STRUCTURE PARAMETERS OF THE BASIC ONE-PORT RESONATOR.

	Resonator 1 (NM-I.H.P.)	Resonator 2 (LV-I.H.P.)
Substrate	50LT	
LT thickness (in wavelength ratio)	600 nm (30.0%)	600 nm (15.0%)
SiO_2 thickness (in wavelength ratio)	667 nm (33.4%)	667 nm (16.7%)
Wavelength	2.0 μm	4.0 μm
Film thickness (in wavelength ratio)	Pt : 0 nm Al : 145 nm (7.25%)	Pt : 120 nm(3.0%) Al : 145 nm (3.13%)
Metallization ratio	0.5	
Electrode overlap length	40.0 μm	
Number of electrode pairs	94	
Number of reflector electrodes	15	
IDT-reflector gap	1.0 μm	2.0 μm

Although this slight degradation of TCF is seen in LV-I.H.P., they are sufficiently with in the allowable range.

V. CONCLUSION

In this paper, we discussed the velocity reduction of the I.H.P. SAW using the heavy Al/Pt electrodes. First, using an FEM simulator, variation of the impedance characteristics with the Pt thickness were calculated, and from the results, variations of the SAW velocity at the resonance and the fractional bandwidth were estimated. In addition, variations of

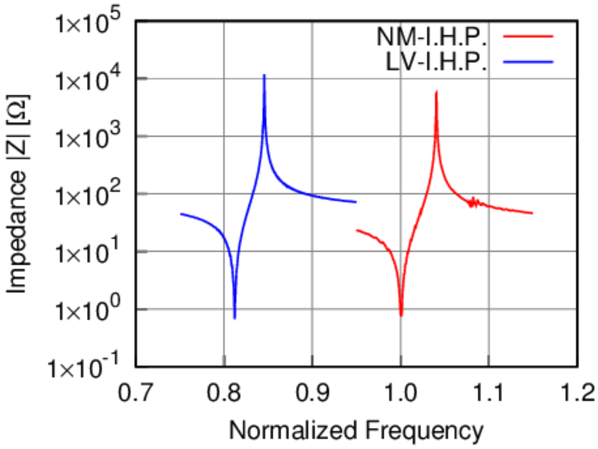

(a) Impedance |Z|

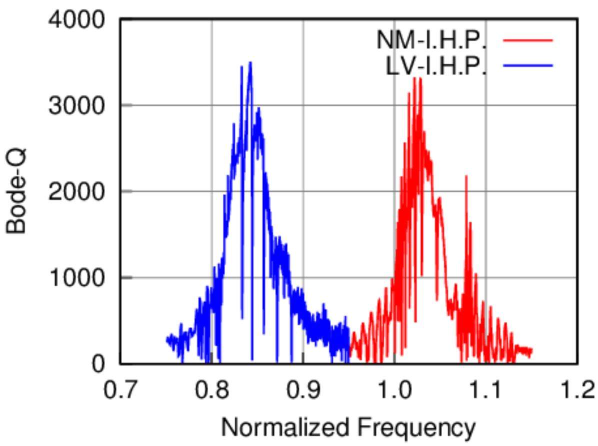

(b) Bode-Q

Fig. 7. Impedance characteristics and Bode-Q of fabricated resonators.

the velocity and the bandwidth with the LT and SiO_2 thicknesses were also estimated. As the result, it is indicated that the SAW velocity decrease with increase of the Pt thickness and, when the Pt thickness is 4.0%, the velocity was expected to be reduced approximately 20% compared with that of conventional I.H.P. SAW. Furthermore, it is also indicated that, although the bandwidth is deteriorated by the increase of the Pt thickness, it can be recovered by reducing the LT and the SiO_2 thicknesses.

Next, on the basis of the estimation results of the FEM simulations, two one-port resonators were fabricated and their velocities, fractional bandwidths, Bode-Qs, and TCFs were evaluated. As the result, it was revealed experimentally that the velocity of I.H.P. SAW was successfully reduced approximately 20% keeping other characteristics by using heavy Pt electrodes and by adjusting the LT and the SiO_2 thicknesses.

TABLE II. MEASURED VALUES OF FABRICATED RESONATORS.

	Resonator 1 (NM-I.H.P.)	Resonator 2 (LV-I.H.P.)
V [m/s]	3791	3076
Fractional bandwidth [%]	4.0	4.1
Qmax	3113	3504
TCF@fr [ppm/°C]	11	15
TCF@fa [ppm/°C]	-12	-13

REFERENCES

[1] T. Takai, H. Iwamoto, Y. Takamine, H. Yamazaki, T. Fuyutsume, H. Kyoya, T. Nakao, H. Kando, M. Hiramoto, T. Toi, M. Koshino, and N. Nakajima, "High-performance SAW resonator on new multilayered dubstrate using $LiTaO_3$ crystal," IEEE Trans. Ultrason., Ferroelectr., Freq. Contr., **64**, 9, 2017, pp. 1382-1389.

[2] D. A. Feld, R. Parker, R. Ruby, P. Bradley, and S. Dong, "After 60 years: A new formula for computing quality factor is warranted," Proc. IEEE Ultrason. Symp., 2008, pp. 431-436.

[3] M. Kadota and S. Tanaka, "Simulation of solidity mounted plate wave resonator with wide bandwidth using 0-th shear horizontal mode in $LiNbO_3$ plate," Japan. J. Appl. Phys., **54**, 2015, 07HD09.

[4] M. Kadota and S. Tanaka, "Near-Zero TCF of HAL SAW Resonator with $LiTaO_3$-on-Quartz Structure," Proc. IEEE Freq. Cont. Symp., 2018, DOI: 10.1109/FCS.2018.8597496.

[5] M. Kadota, Y. Ishii, T. Shimatsu, M Uomoto , and S. Tanaka, "Suprious-free, near-zero-TCF hetero acoustic layer (HAL)SAW resonators using $LiTaO_3$ thin plate on quartz," Proc. IEEE Freq. Cont. Symp., 2018, DOI: 10.1109/ULTSYM.2018.8580111.

[6] J. Hayashi, M. Gomi, M. Suzuki, S. Kakio, H. Suzaki, T. Yonai, K. Kishida, and J. Mizuno, "High-coupling leaky SAWs on $LiTaO_3$ thin plate bonded to quartz substrate," Proc. IEEE Ultrason. Symp., 2017, DOI: 10.1109/ULTSYM.2017.8091566.

[7] N. Naumenko, "Solidly mounted plate mode resonators based on 42°-48°LT cuts: loss mechanisms," Proc. IEEE Ultrason. Symp., 2017, DOI: 10.1109/ULTSYM.2017.8092681.

[8] N. Naumenko, "Suppression of propagation losses in TC SAW resonators using thin plates of $LiTaO_3$ bonded to quartz substrates," Proc. IEEE Ultrason. Symp., 2018, DOI: 10.1109/ULTSYM.2018.8579813.

[9] S. Inoue and M. Solal, "Spurious free SAW resonators on layered substrate with ultra-high Q, high coupling and small TCF," Proc. IEEE Ultrason. Symp., 2018, DOI: 10.1109/ULTSYM.2018.8579852.

[10] M. Mimura, D. Ajima, C. Konoma, and T. Murase, "Small sized band 20 SAW duplexer using low acoustic velocity Rayleigh SAW on $LiNbO_3$ substrate," Proc. IEEE Ultrason. Symp., 2017, DOI: 10.1109/ULTSYM.2017.8092596.

[11] M. Mimura, D. Ajima, and C. Konoma, "SH-Type spurious response free TC-SAW resonators using low acoustic velocity Rayleigh SAW on $LiNbO_3$ substrate," Proc. IEEE Ultrason. Symp., 2018, DOI: 10.1109/ULTSYM.2018.8580200.

[12] T. Takai, H. Iwamoto, Y. Takamine, T. Fuyutsume, T. Nakao, M. Hiramoto, T. Toi, and M. Koshino, "I.H.P SAW technology and its application to microacoustic components," Proc. IEEE Ultrason. Symp., 2018, DOI: 10.1109/ULTSYM.2017.8091876.

[13] K. Hashimoto, Surface Acoustic Wave Devices in telecommunications – modelling and simulation -, Springer Verlag, 2000, Chap.6, pp.163-169.